

Projectile atomic number dependence of the relativistic effect on the K -shell ionization of high Z elements under heavy-ion impact

Y. P. Singh, Ajay Kumar, U. Kadhane, and Lokesh C. Tribedi*
Tata Institute of Fundamental Research, Colaba, Mumbai-400 005, India

D. Trautmann

Institute fuer Theoretische Physik, Universitaet Basel, Klingelbergstrasse 82 CH-4056, Basel, Switzerland
(Received 24 September 2004; revised manuscript received 15 May 2006; published 27 November 2006)

Absolute K -shell ionization cross sections of Sb, Au, and Bi have been measured in collisions with highly charged C, O, and S ions having energies between 2 and 6.25 MeV/ u . The data are presented along with the earlier results with F and Si ions as projectiles. The measured data have been compared with theoretical models based on the semiclassical approximation including relativistic effect and perturbed stationary state approximation including the corrections for energy loss, Coulomb deflection, and relativistic effects. The data were analyzed in term of relativistic effect on K -ionization: its dependence on the projectile atomic number, target atomic number and projectile energy. The present data set along with our recently measured similar data for F and Si ions show that the relativistic effect increases with projectile atomic number and decreases with projectile velocity. A comparison of the experimental data and relativistic calculations, both normalized to nonrelativistic model, show the inadequacy of the theoretical models in describing the relativistic correction on K -shell ionization. For example, the theoretical predictions agree with experimental findings for O ions on Bi while the same theoretical predictions deviate from the experimental results by about a factor of 2 for Si and S on Bi, the theory being higher.

DOI: [10.1103/PhysRevA.74.052714](https://doi.org/10.1103/PhysRevA.74.052714)

PACS number(s): 34.50.Fa

I. INTRODUCTION

The inner shell ionization of atoms in collisions with highly charged ions has been studied over a long period of time. The study of characteristic x rays has gained attention from both atomic and nuclear physicists. The theoretical investigations of these processes have mainly used two approaches, namely, the perturbed stationary state approximation including the corrections for energy loss, Coulomb deflection, and relativistic effects (ECPSSR) [1] and the semiclassical approximation including relativistic effect (SCAR) [2,3]. In the ECPSSR formalism, the target electron is described by the nonrelativistic hydrogenic wave function and relativistic nature of the target electron is accommodated in a phenomenological way. In the semiclassical approach both nonrelativistic (SCA) hydrogenic and relativistic (Dirac) (SCAR) wave functions are used to describe the target electron. Very recently the local plasma approximation (LPA) has also been applied to reproduce the K -ionization cross sections in ion-atom or ion-solid collisions [4,5]. There exist many sets of published data on the K -shell ionization cross sections for relatively low atomic number (Z_t) targets [5–12] for which a nonrelativistic model is good enough.

However, for the heavier elements, the relativistic bound state wave functions are considerably different from those of the nonrelativistic wave functions [13]. Not only the former is larger in magnitude than the latter near the nucleus but also the energy difference between atomic subshells are significant and influence the calculations of ionization cross sections. Hence the relativistic considerations are desirable

for treating the K -shell electrons of heavy elements. Although the ECPSSR successfully predicts the inner shell ionization cross sections for light projectiles such as protons and α -particles (see Ref. [7] for a review) on varieties of targets, it is preferable to check its validity especially for the high Z_t targets for which relativistic correction is important. It is, therefore, customary to have comparative but systematic studies of these two approaches as described above.

To the best of our knowledge, very few such measurements exist on the K -ionization of high Z_t elements [11,14–17] and only a few of them focus on the relativistic effect on K -ionization. These measurements were not aimed at deriving the relativistic effect in a quantitative way. We have already initiated some experimental investigations towards this and reported the K -ionization cross sections of high Z_t elements induced F and Si ions [16,17]. However, to complement these studies here we investigate the dependence of the relativistic effect on the projectile atomic number (Z_p) and Z_t . In order to study the Z_p dependence as well as the energy dependence of relativistic effect we have now measured the cross sections for C, O, and S ions of various energies between 2–6.25 MeV/ amu . To present the data in a coherent fashion, we add some of our recently reported data for F [16] and Si ions [17] on the same set of targets. In addition to comparing the data with the different relativistic models we also make use of the reduced cross sections (i.e., obtained by dividing both the experimental and the theoretical results by the nonrelativistic calculations) in order to explore the applicability of the theoretical models which include the relativistic corrections. In fact, it should be emphasized that this way of comparison shows that in many cases the models are inadequate to explain the relativistic correction.

*Electronic address: lokesh@tifr.res.in

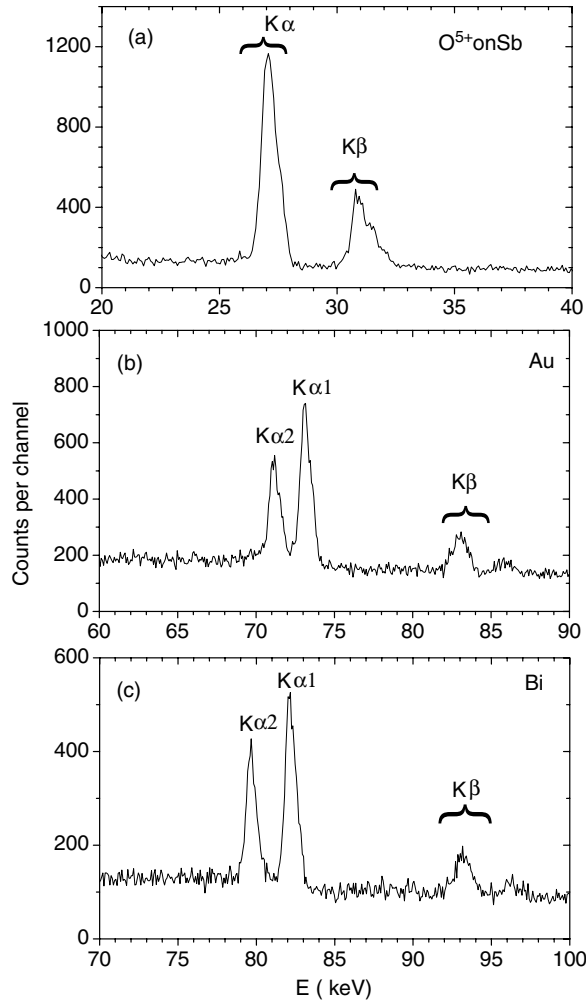


FIG. 1. The K x-ray spectra observed for Sb, Au, and Bi in collisions with 3.375 MeV/amu O^{5+} ions.

II. EXPERIMENTAL DETAILS AND DATA ANALYSIS

The experiment was performed with the 14 MV BARC-TIFR Pelletron accelerator at Mumbai. Highly charged ions of different atomic numbers (Z_p) were used for the measurements. The mass and energy analyzed C, O, and S projectile ions were made to fall on thin targets of Sb, Au, and Bi deposited on carbon backing. The lowest available charge state (q_p) at a given projectile energy was used. For example, q_p was 4+ for carbon ions; 4+, 5+, and 7+ for O ions; and 7+–10+ for S ions based on the beam energy. In the measurements with O and S projectiles, thickness of the targets were 34, 214, 380 $\mu\text{g}/\text{cm}^2$ for Sb, Au, and Bi, respectively. The experiment with C ions was conducted separately and the thickness of these targets were 39, 54, and 133 $\mu\text{g}/\text{cm}^2$, respectively. The carbon backing thickness was about 10 $\mu\text{g}/\text{cm}^2$. Single collision condition was verified for Au target by using several targets of different thickness. However, the K -shell ionization cross sections are too small ~ 1 b (for Au, Bi) and 10–100 b for Sb and one can then see that the single collision conditions are easily satisfied.

The targets were mounted at 90° to the beam direction on a rotatable multiple target holder assembly in an electrically

TABLE I. Intensity ratios, $K\alpha_2$ to $K\alpha_1$ and $K\alpha$ to $K\beta$, for Au and Bi targets. The errors in the data points are about 5%.

Element	$\frac{K\alpha_2}{K\alpha_1}$	$\frac{K\alpha_2}{K\alpha_1}$	Element	$\frac{K\alpha}{K\beta}$	$\frac{K\alpha}{K\beta}$
	theory	measured		theory	measured
Au	0.59	0.63	O/F on Au	3.7	3.7
			Si on Au	3.7	4.67
Bi	0.60	0.64	O/F on Bi	3.64	3.86
			Si on Bi	3.64	4.32

isolated chamber. The vacuum inside the chamber during the experiment was $\sim 10^{-6}$ Torr. The target x rays were detected by high purity Ge detector having an area of 30 mm^2 and thickness of 3 mm. It was mounted outside the vacuum chamber at an angle of 135° with respect to the beam direction. The detector had an energy resolution of 170 eV at 5.9 keV. The x rays from L and M shells were cut down by placing an absorber of suitable thickness in front of the detector window. To measure the thickness of targets *in situ*, a Si surface barrier detector was mounted at an angle of 145° to the beam direction. To obtain the K x-ray production cross sections the x-ray yields were normalized by using the elastically scattered particle spectrum. This takes care of the target thickness and the flux of projectile ions together. However, at relatively higher energies (i.e., above Coulomb barrier) the x-ray yields were divided by the measured target thickness and the collected charges on the Faraday cup. The

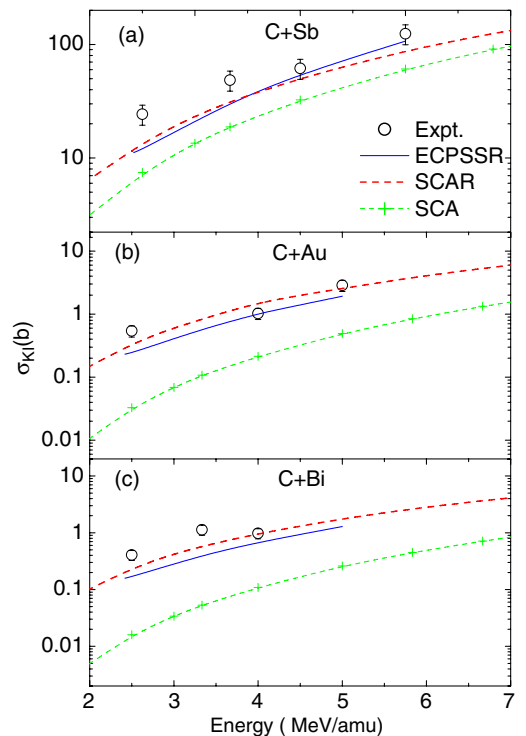


FIG. 2. (Color online) Measured K -shell ionization cross sections (σ_{KI}) for the C ions colliding with (a) Sb, (b) Au, and (c) Bi, plotted along with the different theoretical predictions.

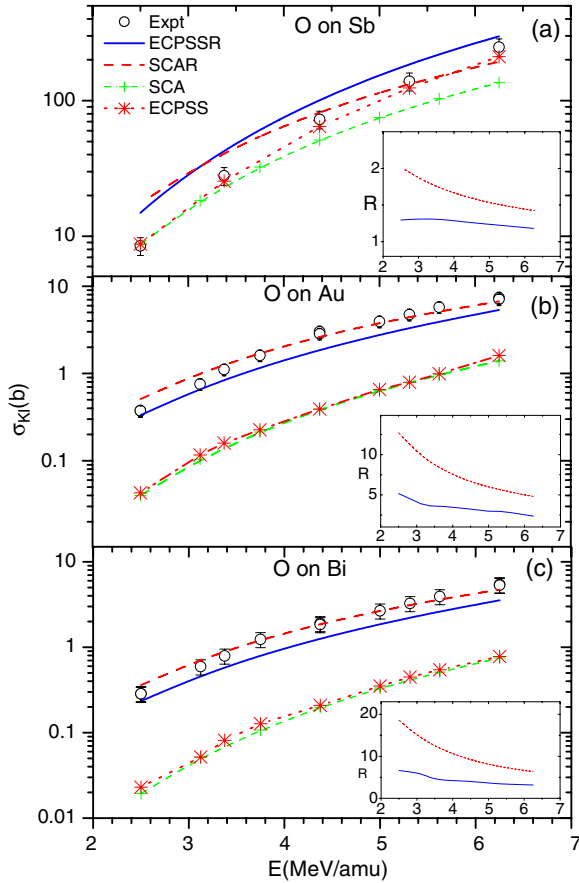


FIG. 3. (Color online) same as in Fig. 2 except for the O ions. The insets show the ratio (R) of the relativistic to nonrelativistic K -shell ionization cross sections obtained using ECPSSR (solid line) and SCAR (dashed line) models.

entire chamber which was electrically isolated was used as the Faraday cup. The intrinsic efficiency of the x-ray detector was measured from time to time using radioactive sources [18] and the experimentally measured efficiency has been used in the extraction of cross section. However, the efficiency is dominated here by the external absorber used. For instance the transmission through absorber is about 24% at

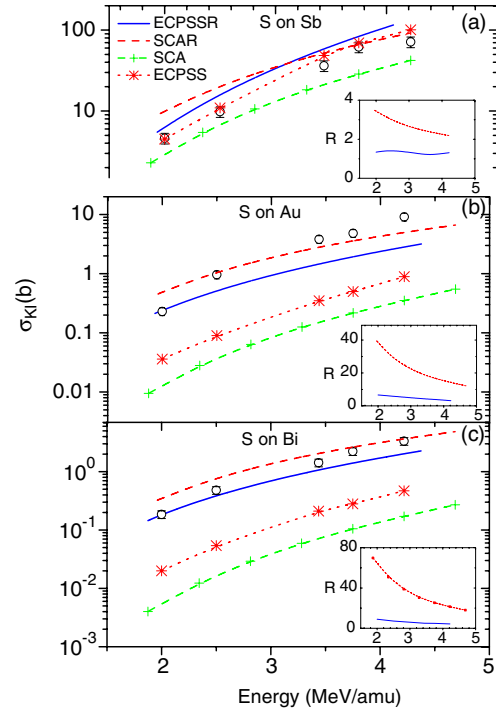


FIG. 4. (Color online) Same as in Fig. 2 except for S as projectile.

27 keV and about 75–78 % between 79 keV ($K\alpha$ line of Bi) and 96 keV ($K\beta$ line of Bi).

Typical x-ray spectra of 3.375 MeV/amu O on all the targets are shown in Figs. 1(a)–1(c). The intensities of the $K\alpha$ and the $K\beta$ group of lines were obtained separately using standard peak fitting program. These intensities were further corrected for efficiency of the detector as well as for the transmission through the absorber used. The measured values of the $K\alpha$ and $K\beta$ intensity ratio for O (or F) on Au or Bi are close to the theoretical values. However, the same ratio for higher atomic number projectiles such as Si on Au or Bi is found to be enhanced (see Table I). It is expected since for Si and S projectiles the ionization cross sections for M - or N -shell electrons (β line originates due to transitions from M - and N -shells) are relatively large. No significant changes in

TABLE II. K ionization cross sections σ_{KI} (in b) of Bi, Au, and Sb induced by C, O, and S ions, respectively. The energy E is in MeV/amu. The errors in the data points are about 15–20 %.

C				O				S			
E	Bi	Au	Sb	E	Bi	Au	Sb	E	Bi	Au	Sb
2.50	0.41	0.542	24.3	2.50	0.285	0.374	8.49	2.00	0.185	0.230	4.61
3.00				3.12	0.593	0.756		2.50	0.481	0.961	9.80
3.33	1.13		48.6	3.37	0.793	1.11	27.9	3.44	1.43	3.81	36.2
4.00	0.98	1.03	61.6	3.75	1.23	1.61		3.75	2.23	4.82	61.8
5.00		2.86	124	4.37	1.90	3.02	72.6	4.22	3.33	9.13	71.3
				5.00	2.67	3.94					
				5.31	3.25	4.73	139				
				5.62	3.93	5.75					
				6.25	5.42	7.39	248				

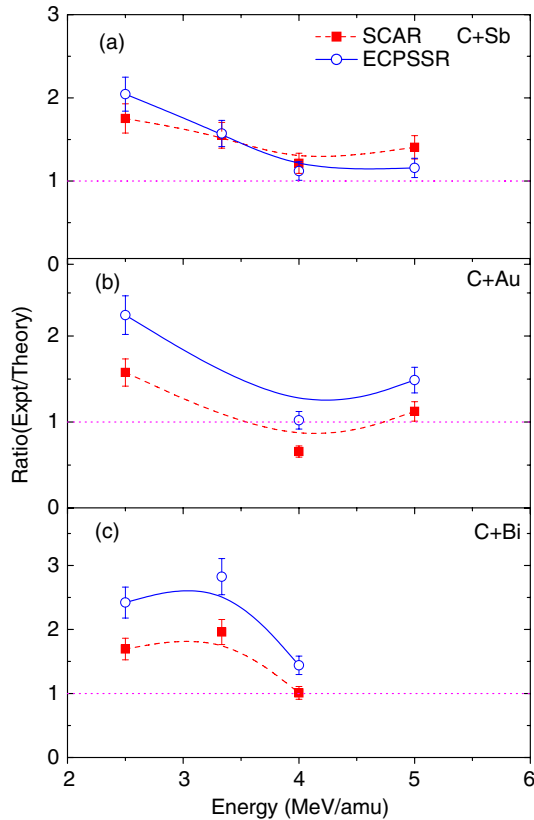


FIG. 5. (Color online) Ratios of the measured data to the calculated cross sections for C ions using the ECPSSR (circles) and the SCAR (squares). The different panels are for different targets. The lines through data points are to guide the eyes. The horizontal line (dash) only to indicate the expected ratio, i.e., 1.0.

the energy of the $K\alpha$ and $K\beta$ transitions (except for Sb) were observed as a function of the beam energy and therefore no significant change in the K -shell fluorescence yield (ω_K) values are expected. As the ω_K is very large, even if there are multiple ionization in the outer shells, for practical purposes, ω_K will not be affected. The K -ionization cross sections (σ_{KI}) were obtained using the single vacancy fluorescence yields tabulated by Krause [19]. These values, being high for the targets studied [ω_K varying between 0.87 (Sb) and 0.96 (Bi)], are not significantly affected by the multiple vacancies in the L and M shells. The overall experimental errors in the measured σ_{KI} were estimated to be about 15–20% arising from the uncertainties in the determination of the intrinsic efficiency of the detector, transmission through absorber, solid angle of the HP(Ge) and SB detectors and the target thickness.

III. RESULTS AND DISCUSSIONS

A. Ionization cross sections

We have compared the present results with the predictions of different theoretical calculations in Figs. 2–4. In these figures, the K -shell ionization cross sections for all the targets (see Table II also), for C, O, and S projectiles have been plotted as a function of projectile energy. In the insets (of

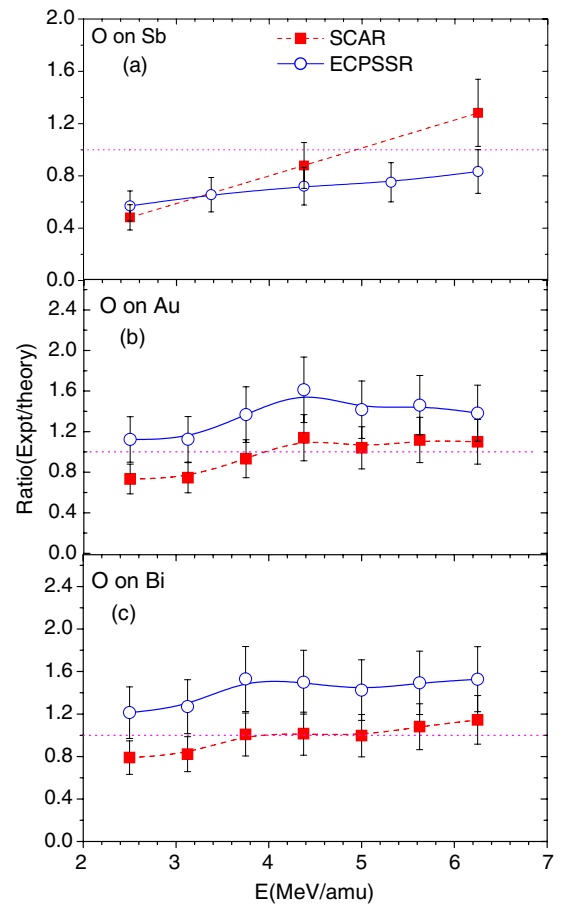


FIG. 6. (Color online) Same as in Fig. 5 except for O as projectile.

Figs. 3 and 4), we have plotted the ratio of cross sections as predicted by the models with and without relativistic corrections. The ratios R thereby symbolize the corrections in the cross sections due to the relativistic effect. The dotted lines (in the insets) represent the ratio R , i.e., $\sigma_{KI}^{SCAR}/\sigma_{KI}^{SCA}$ and the solid line represents $\sigma_{KI}^{ECPSSR}/\sigma_{KI}^{ECPSS}$. The cross sections for Sb, Au, and Bi for carbon ions are qualitatively well reproduced by the SCAR and ECPSSR (Fig. 2). Whereas both the models fall well below the experimental data at low energies, the SCAR model being closer the experimental data as compared to the ECPSSR model. However, the SCA (without relativistic correction) fall much below the experimental data for all the targets, as expected. Obviously, the deviation is least for Sb, since the relativistic correction is less for this element. In general, the ECPSSR underestimates the data throughout the whole energy range and the SCAR underestimates the data in the low energy range and agrees much better at higher energies. This relativistic correction can be estimated by deriving the ratio R with and without including the relativistic correction. According to both the SCAR and ECPSSR models, this ratio R is found to be sensitive to the energy of the incident projectiles as well as the target atomic number. As shown in insets in Figs. 3 and 4, in the SCA model the quantity R decreases as the energy of the incident particle increases and varies between 2 to 1.4 for Sb in the energy range investigated [Fig. 3(a)]. In the extreme case of

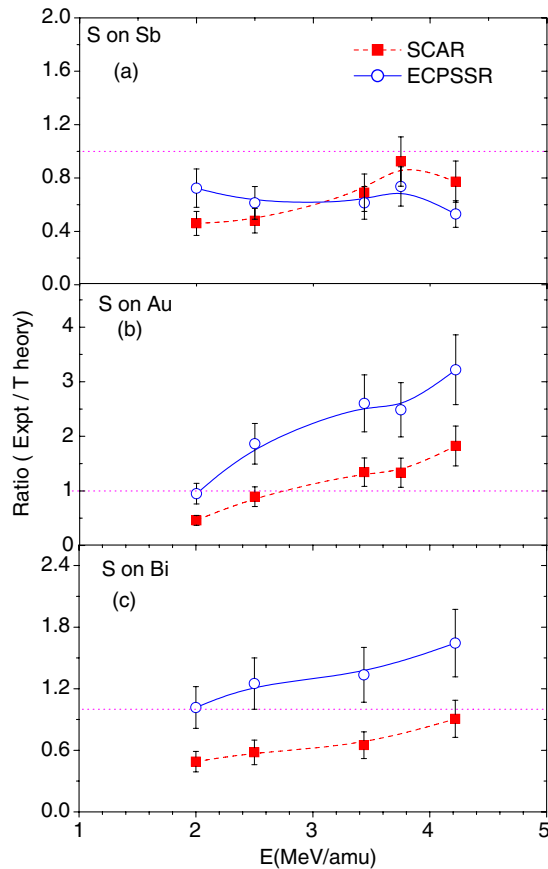


FIG. 7. (Color online) Same as in Fig. 5 except for S projectile.

S on Bi [Fig. 4(c)] it is found to vary between 61 and 21. This ratio is, however, smaller according to the ECPSSR prediction. Even though the relativistic corrections in the calculations are somewhat different yet both the SCAR and ECPSSR explain the experimental ionization data quite well. The SCAR calculations show better agreement as compared to ECPSSR (see Figs. 2–4).

It may be mentioned that for O projectiles, an excellent agreement is found between the data for Au and Bi and the SCAR calculations [Figs. 3(b) and 3(c)]. For Sb target, the SCAR provides good agreement only for higher energies. The ECPSSR overestimates the Sb data and underestimates the Au and Bi data. For S beam again [Figs. 4(b) and 4(c)] the SCAR works better for Au and to some extent for Bi. The ECPSSR gives lower cross section compared to both the data and the SCAR results. For Sb target both models overestimate the data for S ions [Fig. 4(a)]. However the maximum deviations observed for C projectiles are not understood (see Fig. 2).

It may be seen for high Z_t targets such as Au and Bi, the non-relativistic calculations, i.e., ECPSS and SCA agree with each other very well for O projectile [Figs. 3(a)–3(c)] and the SCAR and ECPSSR differ from each other considerably. However for S as projectile even the ECPSS and SCA differ for these high Z_t targets [see Figs. 4(a)–4(c)]. However, this fact could be linked to the magnitude of the relativistic correction as well as the phenomenological way in which this

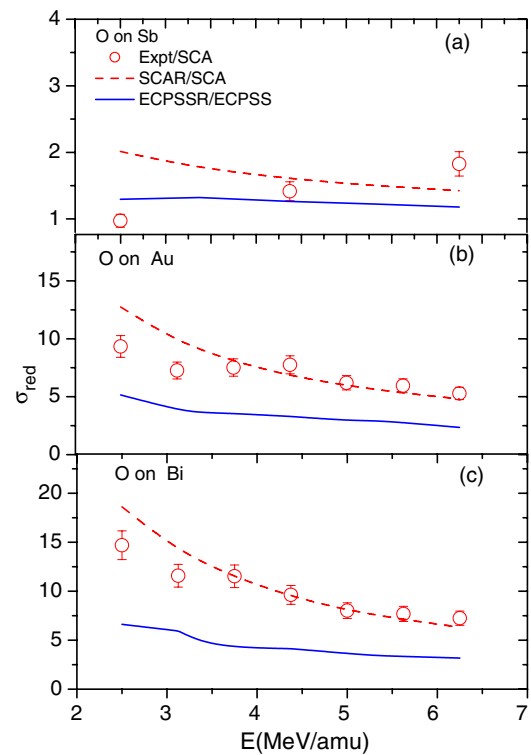


FIG. 8. (Color online) The reduced cross sections, i.e., ratios of the measured cross sections to the SCA (nonrelativistic) cross sections (circles), along with the theoretical ratios, i.e., SCAR to SCA (dashed-line) and ECPSSR to ECPSS (solid line). The different panels represent data for different targets and for O projectiles. As explained in the text this quantity can be approximately the relativistic correction in the σ_{KI} .

effect is introduced in the ECPSSR. To illustrate this aspect further we have plotted (Figs. 5–7) the ratios of the measured cross sections to the theoretical predictions [indicated as “ratio (expt/theory)” in the figures] for all the targets. The expected ratio (i.e., 1.0) is shown by the horizontal line. It is very clear from the Figs. 5–7 that overall the SCAR ratio always remains closer to the expected line compared to the ratios predicted by the ECPSSR. It is also obvious from these three figures that the agreement with the ratios for both the theories are closer to 1.0 in case of O projectile whereas for both the C and S ions the deviation from this line is higher.

B. Relativistic correction

In the present studies the relativistic effects cannot be measured directly. However, the following analysis shows that a quantitative analysis can be made by studying the ratios of the measured data with respect to the theoretical cross sections without relativistic corrections. This is justified since the NR (nonrelativistic) theory predicts almost correctly the cross section of the low Z_t elements, e.g., for Sb. The reduced cross sections σ_{red} are obtained by dividing the experimental cross sections by the nonrelativistic SCA ones which fairly agree with the ionization cross sections for the nonrelativistic case as can be seen from the data for Sb. Also for Sb, the relativistic effect is least expected among all the

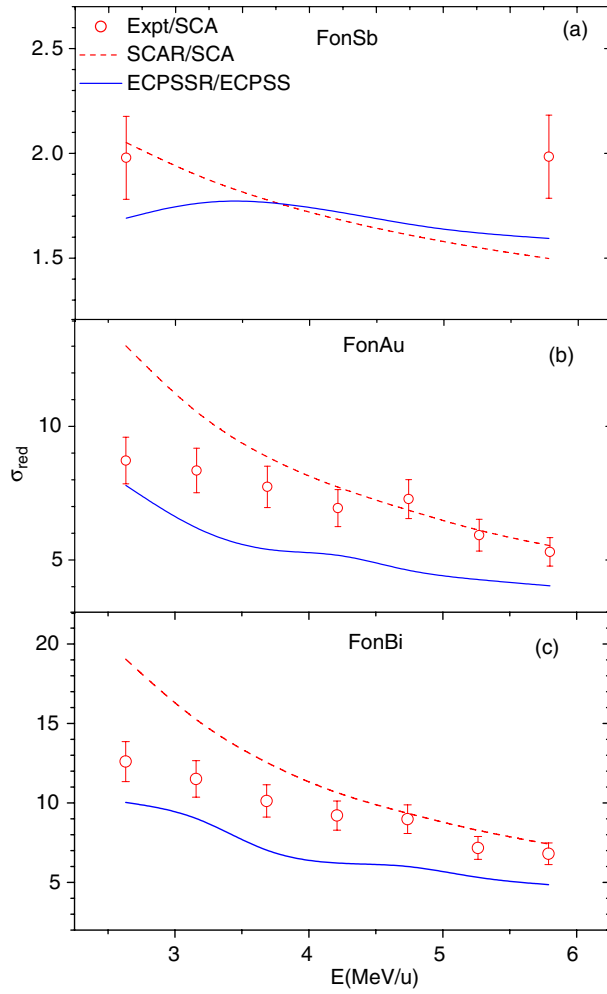


FIG. 9. (Color online) Same as in Fig. 8 except for F as projectile.

targets. The σ_{red} which approximately signify the relativistic effect or correction, are plotted in Figs. 8–11, for different projectiles, namely, O, F, Si, and S for all the targets.

In these graphs there are four common features. (1) The relativistic effect depends on the incident energy of the projectile. It decreases as the energy of the incident projectile increases. However, the decrease is not as sharp as predicted by the SCAR model which overestimates the correction, especially, in the lower energy side. This is a general feature present for all the target/projectile combinations; the deviation gradually increases going from O (Fig. 8) to S (Fig. 11) and it is more drastic for Si (Fig. 10) and S (Fig. 11) projectiles. For S, there is hardly any energy dependence in the data. (2) At a particular energy of the projectile, relativistic effect is higher for the targets with higher atomic numbers Z_t . (3) The relativistic effect also depends on the atomic number Z_p of the projectile. It is higher for higher Z_p for a given energy of the projectiles. (4) For all the targets (except Sb) and projectiles, the relativistic corrections predicted by the ECPSSR are much less than those by the SCAR. (5) In the case of Sb for which the relativistic effect is minimum, the corrections and their energy dependence are generally well reproduced by the ECPSSR model [Figs. 8(a), 9(a), 10(a),

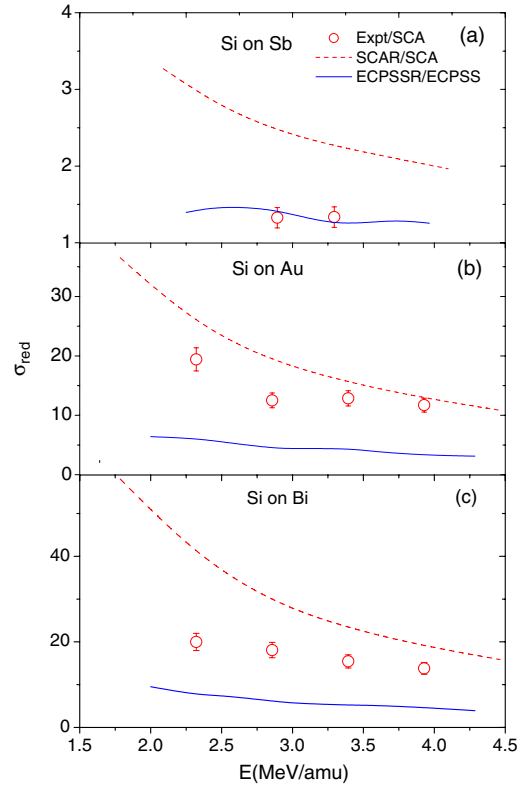


FIG. 10. (Color online) Same as in Fig. 8 except for Si as projectile.

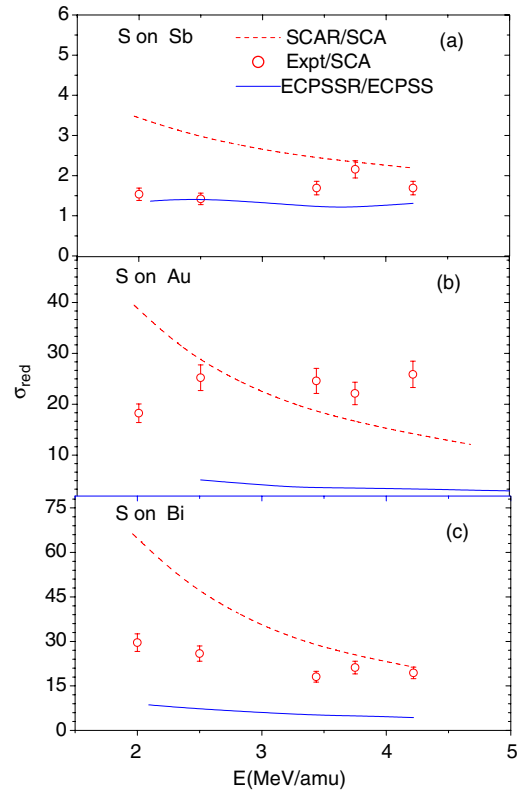


FIG. 11. (Color online) Same as in Fig. 8 except for S as projectile.

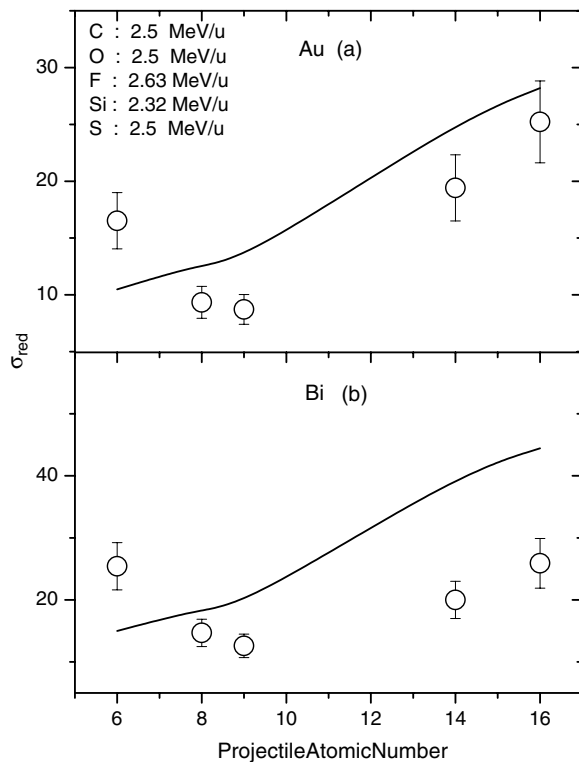


FIG. 12. The Z_p dependence of the reduced cross sections indicating the Z_p dependence of the relativistic effect along with the theoretical prediction (line), i.e., SCAR/SCA.

and 11(a)]. The elements for which the relativistic effect is more pronounced such as for Au and Bi, the SCAR predictions agree quite well with the experimental data at higher energies for O and F [see Figs. 8(b) and 8(c); and Figs. 9(b) and 9(c)]. But at lower energy side the SCAR overestimates the relativistic correction. For example [see Fig. 8(c)], in the case of O on Bi, at 2.5 MeV/amu, the experimental and the SCA correction factors are 14.7 and 18.6, respectively. This discrepancy becomes even more for S on Bi. For example, at 2.5 MeV/amu, the experimental result and the SCAR correction factors are 25.9 and 44.4, respectively, i.e., the SCAR result is 1.7 times higher than the experimental one.

Now the question is why relativistic correction is more at lower energies. At low energies, to ionize the K -shell of a target atom, projectile has to penetrate deep inside the K shell. This causes an enhancement in the binding energy (BE) of the target K -shell electrons since the projectile velocity is much less compared to the orbital velocity of the K -shell electrons [see, e.g., the discussions in the second paragraph on p. 996 and Eq. (37) of Ref. [20]] and thus increasing the orbital velocity. This, in turn, enhances the relativistic correction which leads to higher ionization cross section, as discussed in the introduction. However, the increment in the BE also reduces the ionization cross section which is estimated to be small compared to the enhancement caused by the relativistic effect. For instance, in case of 2.58 MeV/amu F on Au, BE enhancement is only about 5%. So it is obvious that the later process (i.e., relativistic effect) dominates the former (i.e., the BE effect).

Therefore, from the above discussion it can be inferred that the SCAR prediction for the relativistic correction

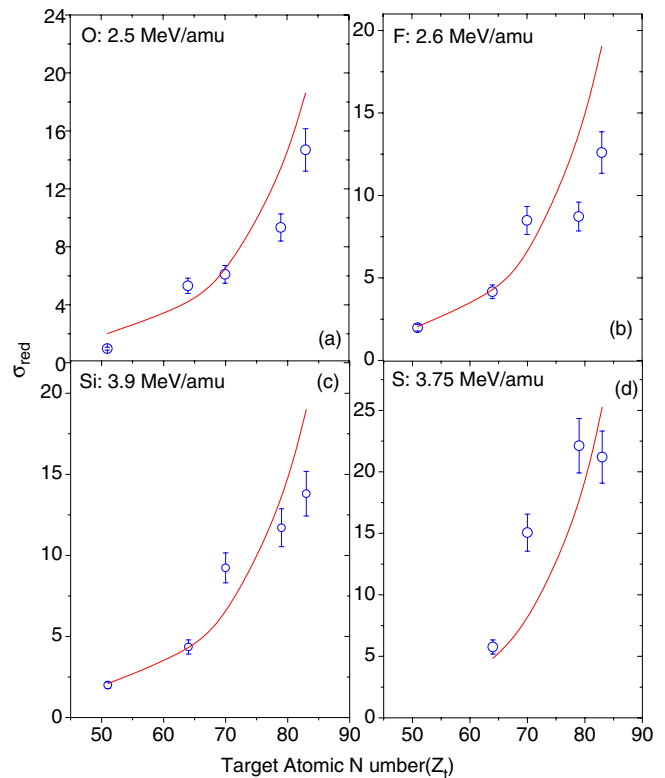


FIG. 13. (Color online) The Z_t dependence of the reduced cross section. The different panels are for four different projectiles at a given energy between 2.5 and 3.9 MeV/amu indicated in the panels. The lines are the corresponding theoretical predictions, i.e., SCAR/SCA.

strongly depends on Z_p and increases with the increment in Z_p . But the Z_p dependence of the measured effect is not as strong as the prediction of the SCAR. This has been shown explicitly in Fig. 12 for Au and Bi. For all the projectiles (except for C), the SCAR prediction for the correction is higher with respect to the data. At the highest Z_p and Z_t studied, the SCAR predicted correction is as high as a factor of 1.7 with respect to the experimental data. The data for C, however, does not follow this general trend which cannot be explained at this stage. However, one can also see that there is a change in the slope of the calculated values at around $Z_p=8$, indicating a possible enhancement for $Z_p < 8$. But the data for C is still too high compared to the prediction. More experimental data would be necessary here. The increment in the relativistic correction for higher Z_p can also be understood in terms of BE enhancement as discussed above.

C. Target atomic number (Z_t) dependence

To investigate more closely the relativistic effect, in Fig. 13, we have plotted the relativistic correction factor (σ_{red}) as a function of Z_t . As above, we find that the SCAR predictions are close to the experimental results. It is clear from these graphs that the SCAR predictions, although agree with the data for the low Z_t elements, deviate for the high Z_t targets for which the relativistic effect is maximum. Therefore, the relativistic effect is overestimated for these high Z_t targets.

For completeness we have also used the data for the Gd and Yb targets in these plots. However, the measurements of these cross sections will be published elsewhere.

IV. CONCLUSIONS

The *K*-shell ionization cross sections of Sb, Au and Bi targets induced by the low and intermediate energy C, O, and S ions have been measured in order to investigate the Z_p dependence of the relativistic effect influencing the ionization cross sections. The relativistic effects on the ionization cross sections are discussed and it is shown that the ratio of the cross sections using relativistic to that using non-relativistic model is quite a large factor. For example, this factor is 4.7 for O on Bi and 29.6 for S on Bi at the lowest energy studied. The relativistic effect decreases with the in-

crement of the projectile energy but increases with the increment in the Z_t . The Z_t dependence of relativistic effect at higher values of Z_t is overestimated by the theoretical calculation. The effect is shown to increase with the Z_p . But the Z_p dependence of the measured effect is not as strong as the prediction of the SCAR. It has been found that the method of using relativistic wave function (as in SCAR) is better than that using relativistic mass of the electron (as in ECPSSR) in the models. Even the SCAR does not give the correct magnitude of the relativistic correction specially at lower energies studied here.

ACKNOWLEDGMENTS

The authors thank the accelerator staff for the smooth operation of the machine.

-
- [1] W. Brandt and G. Lapicki, *Phys. Rev. A* **23**, 1717 (1981), and references therein.
- [2] J. Bang and J. M. Hansteen, *K. Dan. Vidensk. Selsk. Mat. Fys. Medd.* **31**, 13 (1959).
- [3] D. Trautmann and F. Roseel, *Nucl. Instrum. Methods Phys. Res.* **214**, 21 (1983).
- [4] C. C. Montanari, J. E. Miraglia, and N. R. Arista, *Phys. Rev. A* **66**, 042902 (2002).
- [5] U. Kadhane, C. C. Montanari, and L. C. Tribedi, *Phys. Rev. A* **67**, 032703 (2003).
- [6] U. Kadhane, C. C. Montanari, and L. C. Tribedi, *J. Phys. B* **36**, 3043 (2003).
- [7] G. Lapicki, *J. Phys. Chem. Ref. Data* **18**, 111 (1989).
- [8] R. L. Watson, J. M. Blackadar, and V Horvat, *Phys. Rev. A* **60**, 2959 (1999).
- [9] T. J. Gray, P. Richard, R. L. Kauffmann, T. C. Hollowag, R. K. Gardner, G. M. Light, and J. Guertin, *Phys. Rev. A* **13**, 1344 (1976).
- [10] R. K. Gardner, T. J. Gray, P. Richard, C. Schmiedekamp, K. A. Jamison, and J. M. Hall, *Phys. Rev. A* **19**, 1896 (1979).
- [11] G. J. Balster, W. van Huffelen, H. W. Wilschut, D. Chmielewska, and Z. Sujkowski, *Z. Phys. D: At., Mol. Clusters* **2**, 15 (1986).
- [12] L. C. Tribedi, K. G. Prasad, P. N. Tandon, Z. Chen, and C. D. Lin, *Phys. Rev. A* **49**, 1015 (1994).
- [13] T. Mukoyama, *J. Phys. B* **15**, L785 (1982).
- [14] E. Liatard, J. F. Bruandet, F. Glasser, T. U. Chan, G. J. Costa, C. Geradin, C. Heitz, M. Samri, and R. Seltz, *Z. Phys. D: At., Mol. Clusters* **2**, 223 (1986).
- [15] V. L. Kravchuk, A. M. Van den Berg, F. R. R. Fleurot, and H. W. Wilschut (unpublished).
- [16] D. Mitra, Y. Singh, L. C. Tribedi, P. N. Tandon, and D. Trautmann, *Phys. Rev. A* **64**, 012718 (2001).
- [17] Y. P. Singh, U. Kadhane, D. Trautmann, P. N. Tandon, and L. C. Tribedi, *Nucl. Instrum. Methods Phys. Res. B* **212**, 72 (2003).
- [18] L. C. Tribedi and P. N. Tandon, *Nucl. Instrum. Methods Phys. Res. B* **69**, 178 (1992).
- [19] M. O. Krause, *J. Phys. Chem. Ref. Data* **8**, 307 (1979).
- [20] G. Basbas, W. Brandt, and R. Laubert, *Phys. Rev. A* **7**, 983 (1973).